Identification of Novel Hub Genes in Atherosclerosis Induced by Abnormal Endothelial Shear Stress via Bioinformatics Analysis

Guoqi Zhu
Tongji University
Yan Lai
Tongji University
Fei Chen
Tongji University
Jun Qian
Tongji University
Hao lin
Tongji University
Deqiang Yuan
Tongji University
Tongqing Yao
Tongji University
XueBo Liu (lxb70@hotmail.com)
Tongji University

Research Article

Keywords: atherosclerosis, bioinformatics analysis, differentially expressed genes, signaling pathways, hub genes

Posted Date: January 17th, 2022

DOI: https://doi.org/10.21203/rs.3.rs-1253380/v1

Abstract

Background: Abnormal endothelial shear stress (ESS) is a significant risk factor for atherosclerosis (AS); however, the genes and pathways between ESS and AS are poorly understood. Here, we screened hub genes and potential regulatory targets linked to the progression of AS induced by abnormal ESS.

Methods: GSE45225, GSE23289 and GSE43292 were downloaded from the Gene Expression Omnibus (GEO) database. The limma package in R was used to identify differentially expressed genes (DEGs). The common DEGs of GSE45225 and GSE43292 were regarded as low-ESS-AS related genes. Co-DEGs obtained from GSE23289 and GSE43292 were considered as high-ESS-AS related genes. Next, Gene Ontology (GO) annotation and Kyoto Encyclopedia of Genes and Genomes (KEGG) pathway enrichment analysis were conducted. Molecular interaction networks were assembled and their crucial genes were identified using Cytoscape. Our findings were also verified in GSE28829, GSE100927.

Results: A total of 85 low-ESS-AS related genes and 118 high-ESS-AS related genes were identified. FBXO32, ICAM1 and TNFRSF1B were identified as key hub genes and validated in the GSE28829, GSE100927. ROC analysis indicates that FBXO32 (AUC=0.782), ICAM1 (AUC=0.822) and TNFRSF1B (AUC=0.801) could effectively distinguish the atherosclerotic plaque and normal arterial.

Conclusion: We identified ICAM1, TNFRSF1B and FBXO32 as key genes associated with abnormal ESS and AS and may provide potential prevention and treatment target of AS induced by abnormal ESS.

Introduction

Atherosclerosis (AS) and its complications are the leading cause of death and disability in the world and China [1,2]. AS is a long-term chronic inflammatory disease, characterized by subintimal lipid deposition, endothelial injury, inflammatory cell infiltration and atherosclerotic plaque formation [3]. However, the current study cannot fully explain the pathogenesis of AS, which needs further exploration and research. The endothelial cells, a primary layer of protection for vascular, is constantly exposed to a variety of stimuli and insults from circulation [4]. The entire vasculature is exposed to atherosclerotic risk factors, such as hyperglycemia, inflammatory cell infiltration and abnormal blood flow shear stress, which promote the progress of as by inducing endothelial dysfunction, but atherosclerotic plaques tend to form and progress in specific areas of arteries where disordered flow leading to abnormal endothelial shear stress (ESS) [5,6,7].

ESS is a kind of tangential stress generated by the friction of flowing blood upon the endothelial surface of blood vessels, which depends on blood viscosity and velocity gradient at the wall and regulates many functions of endothelium [8]. It has long been recognized that ESS induced by blood flow is recognized independent risk factor for the development of AS [9]. By acting on endothelial cells, flow abnormalities cause shear stress that activates endothelial cells resulting in the activation of endothelial cells, releasing inflammatory factors, and then endothelial dysfunction, which is a significant contribution in the subclinical stages of AS [10,11].

Studies have demonstrated that vulnerable atherosclerotic plaques preferentially develop in regions with low ESS, and the fibrous cap was thinner and the prevalence rates of thin-cap fibroatheroma (TCFA) was higher in the vascular segments with persistently low EES than in other segments [7,12]. At the same time, higher ESS may lead to increased platelet aggregation, plaque erosion and plaque rupture [13,14]. Several studies have shown that abnormal ESS could induce widespread gene expression alterations in ECS that might be involved in the progression of AS [8,15,16,17]. Although the close link between ESS and AS plaque formation has been recognized, the intimate molecular mechanisms remain unclear.

Detection of gene expression by high-throughput sequencing technology is a very powerful tool to reveal the potential genes and biological mechanisms in the process of atherosclerotic plaque formation, which provides a new direction for the discovery of cardiovascular disease mechanism [18]. In this study, bioinformatic technology was used to analyze the relationship between high or low ESS and AS, in order to determine the common molecular mechanism of AS induced by high or low ESS. This approach can be particularly useful to reveal master regulatory or hub genes identified within differential co-expression networks, since hub genes are expected to play a critical role in regulating the expression of several dozens of other genes in the networks. That may provide potential targets for the prevention and treatment of AS.

Results

Identification of DEGs associated with abnormal ESS and AS

In the present research, we searched the GEO database and selected datasets GSE45225, GSE43292 and GSE23289 to identify differentially expressed genes. A schematic diagram of our workflow is shown in Fig.1. We identified 948 DEGs in static (0 dyne/cm^2) compared with physiological ESS (10 dyne/cm^2) from GSE45225 and these 948 DEGs were regarded as LESS-related (low-ESS) genes (Fig. 2A, D). GSE43292 contained samples conducted from pieces of carotid endarterectomy were collected in 32 hypertensive patients, 1314 DEGs were identified from atherosclerotic plaque samples based on the gene expression of control group, which were considered as AS-related genes (Fig. 2B, D). As shown in the UMAP diagram (Fig. 2A), atherosclerotic plaque samples and control group samples are distributed on the right and left respectively, which indicates that there is a good distinction between the two samples. There were 1703 DEGs in high shear stress (75 dynes/cm^2) compared with physiological shear stress (15 dynes/cm^2) from GSE23289 and these 1703 DEGs were regarded as HESS-related (high-ESS) genes (Fig. 2C, D). UMAP analysis showed significant discrimination between samples with abnormal ESS and samples under physiological ESS (Fig. 2A, C).

Identification and functional analysis of co-DEGs between LESS-related genes and AS-related genes

LESS-related genes from GSE45225 and AS-related genes from GSE43292 were integrated, and 85 overlapped genes were obtained from the Venn diagram (Fig. 2D). We define the 85 overlapped genes as LESS-AS-related genes and import it into HIPLOT online tools for further functional enrichment analysis. The Go analysis mainly focused on regulation of peptidyl-serine phosphorylation, regulation of leukocyte mediated immunity, regulation of mast cell degranulation, regulation of blood vessel diameter, membrane raft and ion channel binding. Viral myocarditis and fluid ESS and atherosclerosis are the most relevant KEGG pathway (Fig. 3 and Table 1).

Table 1

GO/KEGG Pathways of LESS-AS-related Genes

Category	Term	P value	Count
BP	regulation of peptidyl-serine phosphorylation	0.005427	7
BP	positive regulation of peptidase activity	0.007351	7
BP	regulation of leukocyte mediated immunity	0.007351	7
BP	regulation of tube diameter	0.007351	6
BP	regulation of tube size	0.007351	6
MF	ion channel binding	0.005024	6
MF	phosphoprotein binding	0.027882	3
MF	peptidase activator activity	0.027882	3
MF	structural constituent of muscle	0.027882	3
MF	cysteine-type endopeptidase regulator activity involved in apoptotic process	0.027882	3
CC	membrane raft	0.000864	9
CC	membrane microdomain	0.000864	9
CC	membrane region	0.000864	9
CC	cell-substrate junction	0.002665	9
CC	focal adhesion	0.049168	7
CC	myofibril	0.049108	5
CC	Z disc	0.049798	4
KEGG	Viral myocarditis	0.04022	4
KEGG	Fluid shear stress and atherosclerosis	0.04768	5

Identification and functional analysis of co-DEGs between HESS-related (High-ESS) genes and AS-related genes

A total of 118 common DEGs in HESS-related genes (GSE45225) and AS-related genes (GSE43292) were identified through Venn diagram online tools and defined as HESS-AS-related genes (Fig. 2D). HIPLOT database was used for further function enrichment analysis. Go analysis showed that negative regulation of transport, regulation of supramolecular fiber organization, negative regulation of myeloid leukocyte

mediated immunity, regulation of secretion, Z disc and I band may be the most relevant pathways. Lysosome is the most relevant KEGG pathway (Fig. 4 and Table 2).

Table 2

GO/KEGG Pathways of HESS-AS-related Genes

Category	Term	P value	Count
BP	negative regulation of transport	2.51E-05	12
BP	regulation of supramolecular fiber organization	0.000336	9
BP	regulation of leukocyte differentiation	0.000299	8
BP	negative regulation of secretion by cell	0.000427	6
BP	bone resorption	0.000531	4
BP	regulation of leukocyte degranulation	0.000161	4
BP	regulation of myeloid leukocyte mediated immunity	0.000364	4
BP	negative regulation of leukocyte degranulation	4.08E-05	3
CC	focal adhesion	0.000728	9
CC	cell-substrate junction	0.000833	9
CC	sarcomere	0.000212	7
CC	myofibril	0.000372	7
CC	contractile fiber	0.000493	7
CC	Z disc	0.000105	6
CC	I band	0.000171	6
CC	actin filament	0.000638	5
CC	main axon	0.000669	4
CC	actin filament bundle	0.001017	4
KEGG	Lysosome	8.82E-05	6

Protein-protein interaction enrichment and hub genes analysis

We further examined the co-expressed genes of HESS-AS-related genes and LESS-AS-related genes and analyzed their expression levels in three datasets (Table 3). In order to further identify the key genes, we introduced 85 LESS-AS-related genes and 118 HESS-AS-related genes into string databases respectively for PPI analysis. Both string interaction networks were imported to Cytoscape and the Molecular Complex Detection (MCODE) algorithm was applied to identify densely connected network components. For the LESS-AS-related genes, we got 16 hub genes in two densely connected gene clusters (Fig. 5A). And 25 hub genes in two clusters were obtained from HESS-AS-related genes (Fig. 5B). Significantly, FBXO32 (also known as Mafbx/Atrogin1), ICAM1_(the intercellular adhesion molecule-1) and TNFRSF1B (tumor necrosis factor receptor 2) were identified as common hub genes, indicating their key roles in abnormal ESS and atherosclerotic plaque (Fig. 5).

Table 3

Expression Levels of Co-expressed Genes in GSE45225, GSE23289 and GSE43292

Co-expressed Genes	GSE45225 Low-ESS vs. Normal ESS (logFC)	GSE23289 High-ESS vs. Normal ESS (logFC)	GSE43292 Plaque vs. Control (logFC)
GIMAP4	-2.11	-3.31	0.75
TMEM47	1.11	0.69	-0.91
FBXO32	1.72	1.09	-0.57
SAMD9L	-1.18	-0.79	0.52
SLC18B1	-1.76	-0.98	0.69
ICAM1	2.47	-0.73	0.75
RASSF2	-1.85	-0.87	0.59
GULP1	1.13	0.88	-0.95
MAP2	1.83	1.32	-0.88
IL13RA2	1.7	1.43	-0.82
PCDH7	1.26	-1.38	-0.80
PRUNE2	-2.12	-0.87	-1.12
KYNU	1.28	-0.80	1.05
TNFRSF1B	-1.95	-0.86	0.71
GEM	1.01	1.14	-0.79
CYYR1	-2.09	-1.02	0.64
NEXN	1.78	0.61	-1.03
LDB2	-2.48	-1.71	0.50
GIMAP4	-2.11	-3.31	0.75

Validation of common hub genes expression in GSE28829 and GSE100927

To confirm and validate the expression of the three common hub genes in atherosclerotic plaque, the expression of the three common hub genes was then validated using GSE28829 and GSE100927. ICAM1 and TNFRSF1B were increased and FBXO32 was decreased in the atheroma plaque compared with

control tissue in GSE43292 and GSE100927 (Fig. 6A, B). Further mRNA analysis in GSE28829 showed that ICAM1 and TNFRSF1B were increased and FBXO32 was decreased in advanced plaques compared to early plaques, which were consistent with our previous findings (Fig. 6C).

Receiver operating characteristic (ROC) curve analyses of the common hub genes in atherosclerotic disease

ROC curve analyses were conducted to assess the ability of common hub genes to distinguish samples of atherosclerotic plaque from normal arterial. Their ROC curves indicated that the expression of FBXO32(AUC=0.782) (Fig. 7A), ICAM1(AUC=0.822) (Fig. 7B) and TNFRSF1B(AUC=0.801) (Fig. 7C) could effectively distinguish the atherosclerotic plaque and normal arterial (AUC >0.7). Furthermore, the combination of three indexes improved the sensitivity and specificity of prediction accuracies (AUC = 0.824) (Fig. 7D). Moreover, we confirmed the powerful discrimination ability of these three mRNA in GSE100927 with an AUC of 0.715 in FBXO32 (Fig. 8A), AUC of 0.913 in ICAM1 (Fig. 8B), and AUC of 0.756 in TNFRSF1B (Fig. 8C). The expression of FBXO32(AUC=0.760) (Fig. 8D), ICAM1_(AUC=0.909) (Fig. 8E) and TNFRSF1B_(AUC=0.947) (Fig. 8F) also demonstrated strong discriminatory power for advanced atherosclerotic plaques in GSE28829.

Discussion

It is known that vascular endothelial cells (ECs) first sense ESS changes, a known activator of ECs that contributes to atherosclerotic plaque formation mainly in bifurcated vessels such as carotid arteries [14,19,20]. In fact, vascular injury and endothelial dysfunction induced by abnormal ESS are often regarded as a hallmark for AS. Continuous low-grade injury to ECs, induced by disturbed flow at arterial branch points and curvatures, could lead to apoptosis and inflammation, causing endothelial cell dysfunction which was considered critical initiating step in the pathogenesis of AS–. Therefore, further studies are necessary to fully understand the potential mechanisms. In the present study, we focused on alterations in ECs gene expression that result from abnormal blood flow shear forces, which are capable of inducing atherosclerotic plaque progression.

ECs express a unique transcriptional profile under very high ESS, which is known to induce extracellular matrix synthesis and expansive arterial remodeling [15,21]. In addition, excessively low blood flow shear is able to induce the change of the gene expression pattern of ECs, leading to the progression of atherosclerotic lesions [6,16]. Studies have reported that shear stress may regulate the growth characteristics of vascular smooth muscle cells by altering the EC and inflammatory regulation, and then contribute the formation of atherosclerotic lesions [15,17]. Based on the above researches, we further studied the specific molecular mechanism of atherosclerotic plaque progression induced by abnormal blood flow shear stress using bioinformatics technology.

Previous studies have shown that physiological shear stress is in the ranges of 1-50 dyne/cm^2 [22,23]. In this study, we analyzed the changes of gene expression profiles of ECs exposed to low, physiological and high (0,10 or 15,75 dyne/cm^2) shear stress (GSE45225 and GSE23289). Using bioinformatics techniques, we identified 1141 LESS-related DEGs from GSE45225 and 1844 HESS-related DEGs from GSE23289. From GSE43292, we got 1481AS-related DEGs between AS tissues and control samples.

To search for preventive and therapeutic targets for AS induced by ESS, three co-hub genes were screened out: FBXO32, ICAM1 and TNFRSF1B. In addition, the expression of these genes in advanced atherosclerotic plaques was also studied. Compared with their expression levels in control tissues, ICAM1 and TNFRSF1B expression increased in atherosclerotic plaques while FBXO32 expression decreased. ROC analysis demonstrates that the differential expression of these three genes had reliable value in differentiating plaques and even identifying advanced stages. The three promising mRNAs, proposed by this study, that could provide some clues to reveal the potential molecular mechanism of abnormal ESS and AS. These data will also help to predict the clinical deterioration of patients with advanced and ruptured AS plaque, and may also provide potential targets for treatment.

ICAM1, a member of the immunoglobulin family, is expressed on cell surface and mediates the adhesion of the cell to other cells or to the extracellular matrix[24,25]. Our analysis demonstrates that excessively low blood flow shear forces produce a significant increase in ICAM1 expression in ECs. In atherosclerotic plaques, increased ICAM1 expression was detected. Ishibazawa et al. also proved that LSS could promote the expression of proinflammatory genes ICAM1[26]. Earlier studies showed that ICAM1 was barely expressed on the cell surface in a normal endothelium or without proinflammatory stimuli [27]. Under pathological conditions, increased expression of ICAM1 can mediate endothelial cell activation, causes enhanced interaction of ECs with leukocytes. This is followed by a stepwise recruitment of leukocytes, rolling, activation, migration and adhesion on the vascular basement membrane, which in turn induce atherosclerotic plaque formation [28,29]. The AS risk in communities (ARIC) study indicate that plasma levels of ICAM1 may serve as molecular markers for AS and the development of coronary heart disease (CHD) [30]. In patients with coronary slow flow (CSF), ICAM1 K allele plays an important role in the pathogenesis of AS, which is related to the decrease of coronary blood flow. Both above studies and results of our analysis suggest that ICAM1 plays a central role in endothelial dysfunction. Combined with our research, it is reasonable to suggest that ICAM1 plays an important role in AS progression resulting from abnormal ESS and might be a possible target for AS prevention and treatment.

Tumor necrosis factor (TNF) is a pleiotropic cytokine that involved in the pathogenesis of inflammatory diseases such as endothelial injury and AS. TNF exerts its biological functions by binding to its two different receptors, the TNF receptor 1 (TNFR1, TNFRSF1A) and the TNF receptor 2 (TNFR2, TNFRSF1B), which differ in structure, expression patterns and signaling pathways that they induce [31,32].TNFRSF1A is expressed in most cell types, while TNFRSF1B appears to function exclusively in immune and ECs [33]. Some studies have shown that TNFRSF1B mainly triggers tissue repair and regeneration, whereas TNFRSF1A promotes apoptosis or inflammation [34]. In the study by Luo, Y et al. have shown that overexpression of TNFRSF1B in ECs can reduce cell death induced by ischemia-reperfusion and promote

the proliferation of ECs, vasoformation and vessel maturation after injury [35]. Our analysis showed that the abnormal increase or decrease of ESS could inhibit the expression of TNFRSF1B in ECs. These results have shown that TNFRSF1B plays a critical role in mediating endothelial dysfunction induced by abnormal ESS.

It is interesting to note that the expression of TNFRSF1B was increased in atherosclerotic plaque tissue. We suspected that in the early stages of endothelium dysfunction, abnormal ESS promotes endothelial cell death, inhibits endothelial cell proliferation and neovascularization after injury, and finally leads to endothelial dysfunction by inhibiting the expression of TNFRSF1B in ECs [35]. Moreover, the high expression of TNFRSF1B in atherosclerotic plaque tissue contributes to the progression, rupture or erosion of atherosclerotic plaques by stimulating leucocyte adhesion and inflammatory cell recruitment [36]. In addition, ROC analysis indicates that the expression level of TNFRSF1B represented highly efficient in discriminate AS (AUC = 0.801). Previous studies have also revealed the association of the TNFRSF1B allele with increased risk of development of myocardial infarction [37,38]. We can see through our studying and analyzing**,** that TNFRSF1B might be a potential new atherosclerosis prevention and therapeutic target.

FBXO32 was originally identified as a muscle-specific ubiquitin-E3 ligase, and further study indicated that it plays a key role in heart development and muscle homeostasis [39]. Serum starvation and hypoxia can also induce the expression of this gene, which can regulate apoptosis [40,41]. Another study showed that the deficiency of FBXO32 can lead to cardiomyopathy due to impaired autophagy [42]. Autophagy and apoptosis may be the potential mechanisms by which FBXO32 promotes the progression of AS. Nevertheless, the above researches on FBXO32 were mainly focused on cardiomyocytes and cardiac function. Currently, the role of FBXO32 in endothelial injury and AS are still poorly investigated, and the underlying mechanism is poorly understood. Through the analysis of datasets GSE23289 and GSE45225, we found that abnormal ESS can lead to the overexpression of FBXO32 in ECs. Further studies showed that, compared with the control group, the expression of FBXO32 in atherosclerotic plaque was significantly decreased and the ROC curves confirmed that FBXO32 could distinguish the AS state. Subsequent cellular experiments also demonstrated a significant decrease in FBXO32 expression in foam cells. Although the exact mechanisms still need to be identified, FBXO32 may represent an important target for prevention and treatment of AS.

We think that a series of genome-wide, unbiased screens for identifying hub genes would be of considerable value for revealing mechanisms and potential therapeutic targets. Our present findings have demonstrated that FBXO32, ICAM1 and TNFRSF1B play vital roles in abnormal ESS and endothelial dysfunction. These genes may warrant as valuable targets for prevention and treatment of AS induced by abnormal ESS.

This study has some limitations. First, due to the small sample size of datasets GSE45225 and GSE23289, larger studies are required to confirm our findings. Second, different sample sources and detection microarray platforms may contribute to some of the differences in gene expression. In addition,

we verified the expression of these genes only in vitro assays, and no clinical specimens were obtained for further validation. In the future, to verify our hypothesis, more research that includes larger samples, randomized trial designs, further mechanistic studies, and even more clinical trials is needed.

Conclusions

This preliminary study provides evidence linking altered ESS to AS and atherosclerotic plaques. Specifically, we identified ICAM1, TNFRSF1B and FBXO32 as key genes associated with abnormal ESS and AS, and initially explored the roles of these genes in endothelial dysfunction and AS, thus highlighting the possibility of new preventive and therapeutic strategies for AS by targeting these genes. ICAM1 and TNFRSF1B were correlated with inflammation, there-by promoting endothelial dysfunction and plaque progression, and it may even contribute to plaque rupture as it facilitates the recruitment of immune cells. Whereas the role played by FBXO32 in AS is not clear, we speculate that its expression may affect AS by regulating autophagy or apoptosis.

Materials And Methods

Microarray datasets

The GEO database (https://www.ncbi.nlm.nih.gov/geo), fully known as gene expression omnibus, incorporates high-throughput gene expression data proposed by global research institutions [43]. In the present research, to investigate the relationship between abnormal ESS and AS, we searched the GEO database and selected datasets GSE45225, GSE43292 and GSE23289. GSE45225 contains the gene expression dataset of human umbilical vein endothelial cells (HUVECs) submitted to static and physiological (0 and 10 dyne/cm^2) shear stress in laminar flow bioreactor system for 24h [44,45]. In GSE43292, carotid intima samples were collected from 32 patients with hypertension, including 32 corresponding atherosclerotic samples and 32 normal carotid samples [46]. In GSE23289, HUVECs were cultured for 24 hours under laminar shear stress of either 15 dynes/cm^2 (physiological shear stress) or 75 dynes/cm^2 (high shear stress) and transcriptomics and related functional analyses were used to assess the effect of high shear stress on ECs [47]. Several published data sets were used to validate the differential expression of key genes in atherosclerotic tissue. The GSE28829 dataset consists of 13 early and 16 advanced human carotid atherosclerotic plaque samples [48]. And GSE100927 contains data on atherosclerotic lesions and control arteries without atherosclerotic lesions obtained from carotid, femoral and infra-popliteal arteries [49]. Based on workflow, we analyzed the five datasets, screened and verified hub genes (Fig. 1).

Identification of DEGs

Datasets were downloaded from the NCBI-GEO public database and loaded into R software. Differential gene expression was performed with limma package with |log FC| > 0.5 and adjusted P value

<_0.05 [50]. UMAP analysis was used to detect the discrimination between different types of samples. For the GSE45225 dataset, the DEGs of static (0 dyne/cm^2) compared with physiological ESS (10 dyne/cm^2) were identified. From the GSE43292, we got the DEGs between plaque and control samples. Both DEGs were introduced into the online tool (http://bioinformatics.psb.ugent.be/webtools/Venn) to obtain common DEGs (co-DEGs) of GSE45225 and GSE43292. For the GSE23289, we compared the gene expression of HUVEC submit to high ESS (75 dynes/cm^2) and physiological ESS (15 dynes/cm^2) to identify the DEGs and the co-DEGs of GSE23289 and GSE43292 were obtained.

Functional enrichment analysis of DEGs

In order to reveal the underlying biological functions of genes related to abnormal ESS and atherosclerotic plaque, both co-DEGs were imported into the HIPLOT database (https://hiplot.com.cn/) for Gene Ontology (GO) and Kyoto Encyclopedia of Genes and Genomes (KEGG) enrichment analysis [51]. GO is an international standardized gene functional classification system. GO terms were divided into three gene set libraries: Biological Process (BP), Cellular Component (CC) and Molecular Function (MF) [52,53]. And KEGG describes the pathways enriched in gene sets [54].

Identification of hub Genes

Both co-DEGs lists were loaded into the STRING database for Protein-protein Interaction (PPI) enrichment analysis [55]. According to the PPI network, the MCODE algorithm in Cytoscape software has been applied to identify hub genes [56]. Hub genes of two PPI network were intersected to get common hub genes.

Receiver operating characteristic (ROC) curve for diagnostic effectiveness evaluation of common hub genes

To evaluate the diagnostic effectiveness evaluation of hub genes, samples were divided into AS and control groups. The pROC package and ggplot2 package were used to draw ROC curve and calculate the area under the curve (AUC) to evaluate the capability and sensitivity of common hub genes to distinguish atherosclerotic samples from control group [57,58]. According to previous studies, AUC = 0.5 indicates no evaluation efficacy, 0.7 ≤ AUC <0.8 indicates acceptable evaluation efficacy, 0.8 ≤ AUC<0.9 represents excellent evaluation efficacy and AUC ≥ 0.9 means outstanding evaluation efficacy [59].

Abbreviations

ESS: Endothelial shear stress; AS: Atherosclerosis; GEO: Gene Expression Omnibus; DEGs: Differentially expressed genes; GO: Gene Ontology; KEGG: Kyoto Encyclopedia of Genes and Genomes; TCFA: Thin-cap fibroatheroma; LESS: Low endothelial shear stress; HESS: High endothelial shear stress; PPI: Protein-

protein interaction; MCODE: Molecular Complex Detection algorithm; ROC: Receiver operating characteristic; AUC: Area under the curve; ECs: Endothelial cells; ARIC: AS risk in communities study; CHD: Coronary heart disease; CSF: coronary slow flow; TNFRSF1A: Tumor necrosis factor receptor 1; TNFRSF1B: Tumor necrosis factor receptor 2; HUVECs: Human umbilical vein endothelial cells; BP: Biological Process; CC: Cellular Component; MF: Molecular Function.

Declarations

Acknowledgments

The authors acknowledge TCGA and GEO database for providing their platforms and contributors for uploading their meaningful datasets. We authors acknowledge the online tools of HIPLOT (https://hiplot.com.cn/) and XIANTAO (https://www.xiantao.love/) for facilitating our data analysis.

Authors' contributions

GZ was the principal investigator, analyzed the data and drafted the manuscript. FC contributed to the idea of the manuscript. HL and JQ designed and drew the figures. DY and TY wrote a part of the manuscript. XL and YL directed the writing. All authors read and approved the final manuscript.

Funding

This work was supported by the National Natural Science Foundation of China (Grant No.81670403), Grant of Shanghai Science and Technology Committee (NO. 18411950300, 19XD1403300, and 19411963200).

Availability of data and materials

The datasets analyzed in this study are available from the corresponding authors on request.

Conflict of interest

The authors declare no competing interests.

Ethics approval and consent to participate

TCGA and GEO belong to public databases. The patients involved in the database have obtained ethical approval. Users can download relevant data for free for research and publish relevant articles. Our study is based on open source data, so there are no ethical issues and other conflicts of interest.

Consent for publication

Not applicable.

Competing interests

All authors declare that there are no conficts of interest.

Author details

[1] Department of Cardiology, Tongji Hospital, School of Medicine, Tongji University, No.389, Xincun Rd, Putuo District, Shanghai 200065, People's Republic of China.

References

1. Yang X, Li J, Hu D, Chen J, Li Y, Huang J, et al. Predicting the 10-Year Risks of Atherosclerotic Cardiovascular Disease in Chinese Population: The China-PAR Project (Prediction for ASCVD Risk in China). Circulation. 2016; 134(19):1430-1440.
2. Kruk ME, Gage AD, Joseph NT, Danaei G, Garcia-Saiso S, Salomon JA. Mortality due to low-quality health systems in the universal health coverage era: a systematic analysis of amenable deaths in 137 countries. Lancet. 2018; 392(10160):2203-2212.
3. Brown RA, Shantsila E, Varma C, Lip GY. Current Understanding of Atherogenesis. Am J Med. 2017; 130(3):268-282.
4. Ma ZY, Yu YR, Badea CT, Kovacs JJ, Xiong XY, Comhair S, et al. Vascular Endothelial Growth Factor Receptor 3 Regulates Endothelial Function Through beta-Arrestin 1. Circulation. 2019; 139(13):1629-1642.
5. Pi X, Xie L, Patterson C. Emerging Roles of Vascular Endothelium in Metabolic Homeostasis. Circ Res. 2018; 123(4):477-494.
6. Chatzizisis YS, Coskun AU, Jonas M, Edelman ER, Feldman CL, Stone PH. Role of endothelial shear stress in the natural history of coronary atherosclerosis and vascular remodeling - Molecular, cellular, and vascular behavior. Journal of the American College of Cardiology. 2007; 49(25):2379-2393.
7. Vergallo R, Papafaklis MI, Yonetsu T, Bourantas CV, Andreou I, Wang Z, et al. Endothelial shear stress and coronary plaque characteristics in humans: combined frequency-domain optical coherence tomography and computational fluid dynamics study. Circ Cardiovasc Imaging. 2014; 7(6):905-911.
8. Gregory F. Role of mechanical stress and neutrophils in the pathogenesis of plaque erosion. Atherosclerosis. 2021; 318(60-69.
9. Cheng C, Tempel D, van Haperen R, van der Baan A, Grosveld F, Daemen MJ, et al. Atherosclerotic lesion size and vulnerability are determined by patterns of fluid shear stress. Circulation. 2006;

113(23):2744-2753.

10. Glagov S, Zarins CK. Compensatory Enlargement of Human Atherosclerotic Coronary-Arteries - Reply. New England Journal of Medicine. 1987; 317(25):1604-1604.
11. Korkmaz H. Brachial artery intima-media thickness/The relation of intima-media thickness with endothelial function and left ventricular mass index. Anatolian Journal of Cardiology. 2010; 10(5):467-468.
12. Abe S, Nishino S, Sakuma M, Inoue T. Low Endothelial Sheer Stress- A Silent Killer. Circ J. 2019; 83(6):1197-1199.
13. Chatzizisis YS, Baker AB, Sukhova GK, Koskinas KC, Papafaklis MI, Beigel R, et al. Augmented expression and activity of extracellular matrix-degrading enzymes in regions of low endothelial shear stress colocalize with coronary atheromata with thin fibrous caps in pigs. Circulation. 2011; 123(6):621-630.
14. Koskinas KC, Feldman CL, Chatzizisis YS, Coskun AU, Jonas M, Maynard C, et al. Natural history of experimental coronary atherosclerosis and vascular remodeling in relation to endothelial shear stress: a serial, in vivo intravascular ultrasound study. Circulation. 2010; 121(19):2092-2101.
15. Qi YX, Han Y, Jiang ZL. Mechanobiology and Vascular Remodeling: From Membrane to Nucleus. Adv Exp Med Biol. 2018; 1097(69-82.
16. Cunningham KS, Gotlieb AI. The role of shear stress in the pathogenesis of atherosclerosis (vol 85, pg 9, 2005). Laboratory Investigation. 2005; 85(7):942-942.
17. Russo TA, Stoll D, Nader HB, Dreyfuss JL. Mechanical stretch implications for vascular endothelial cells: Altered extracellular matrix synthesis and remodeling in pathological conditions. Life Sci. 2018; 213(214-225.
18. Tan XW, Zhang XT, Pan LL, Tian XX, Dong PZ. Identification of Key Pathways and Genes in Advanced Coronary Atherosclerosis Using Bioinformatics Analysis. Biomed Research International. 2017; 2017(
19. Stone PH, Coskun AU, Kinlay S, Clark ME, Sonka M, Wahle A, et al. Effect of endothelial shear stress on the progression of coronary artery disease, vascular remodeling, and in-stent restenosis in humans: in vivo 6-month follow-up study. Circulation. 2003; 108(4):438-444.
20. Tsaousi A, Mill C, George SJ. The Wnt pathways in vascular disease: lessons from vascular development. Curr Opin Lipidol. 2011; 22(5):350-357.
21. Dolan JM, Sim FJ, Meng H, Kolega J. Endothelial cells express a unique transcriptional profile under very high wall shear stress known to induce expansive arterial remodeling. Am J Physiol Cell Physiol. 2012; 302(8):C1109-1118.
22. Silver AE, Vita JA. Shear-stress-mediated arterial remodeling in atherosclerosis: too much of a good thing? Circulation. 2006; 113(24):2787-2789.
23. Chiu JJ, Chien S. Effects of disturbed flow on vascular endothelium: pathophysiological basis and clinical perspectives. Physiol Rev. 2011; 91(1):327-387.

24. Burgos V, Paz C, Saavedra K, Saavedra N, Foglio MA, Salazar LA. Drimenol, isodrimeninol and polygodial isolated from Drimys winteri reduce monocyte adhesion to stimulated human endothelial cells. Food and Chemical Toxicology. 2020; 146(
25. Inwald D, Davies EG, Klein N. Demystified ... Adhesion molecule deficiencies. Journal of Clinical Pathology-Molecular Pathology. 2001; 54(1):1-7.
26. Ishibazawa A, Nagaoka T, Yokota H, Ono S, Yoshida A. Low shear stress up-regulation of proinflammatory gene expression in human retinal microvascular endothelial cells. Experimental Eye Research. 2013; 116(308-311.
27. Yan J, Nunn AD, Thomas R. Selective induction of cell adhesion molecules by proinflammatory mediators in human cardiac microvascular endothelial cells in culture. International Journal of Clinical and Experimental Medicine. 2010; 3(4):315-331.
28. Blankenberg S, Barbaux S, Tiret L. Adhesion molecules and atherosclerosis. Atherosclerosis. 2003; 170(2):191-203.
29. Rahman A, Fazal F. Hug Tightly and Say Goodbye: Role of Endothelial ICAM-1 in Leukocyte Transmigration. Antioxidants & Redox Signaling. 2009; 11(4):823-839.
30. Hwang SJ, Ballantyne CM, Sharrett AR, Smith LC, Davis CE, Gotto AM, et al. Circulating adhesion molecules VCAM-1, ICAM-1, and E-selectin in carotid atherosclerosis and incident coronary heart disease cases - The atherosclerosis risk in communities (ARIC) study. Circulation. 1997; 96(12):4219-4225.
31. Wajant H, Pfizenmaier K, Scheurich P. Tumor necrosis factor signaling. Cell Death and Differentiation. 2003; 10(1):45-65.
32. Loetscher H, Schlaeger EJ, Lahm HW, Pan YC, Lesslauer W, Brockhaus M. Purification and partial amino acid sequence analysis of two distinct tumor necrosis factor receptors from HL60 cells. J Biol Chem. 1990; 265(33):20131-20138.
33. Faustman DL, Davis M. TNF receptor 2 and disease: autoimmunity and regenerative medicine. Frontiers in Immunology. 2013; 4(
34. Aggarwal BB. Signalling pathways of the TNF superfamily: A double-edged sword. Nature Reviews Immunology. 2003; 3(9):745-756.
35. Luo Y, Xu Z, Wan T, He Y, Jones D, Zhang HF, et al. Endothelial-Specific Transgenesis of TNFR2 Promotes Adaptive Arteriogenesis and Angiogenesis. Arteriosclerosis Thrombosis and Vascular Biology. 2010; 30(7):1307-U1372.
36. Gitlin JM, Loftin CD. Cyclooxygenase-2 inhibition increases lipopolysaccharide-induced atherosclerosis in mice. Cardiovascular Research. 2009; 81(2):400-407.
37. Markoula S, Chatzikyriakidou A, Giannopoulos S, Odysseas K, Markou S, Vemmos K, et al. Association of TNF-857C>T, TNFRSF1A36A>G, and TNFRSF1B676T>G Polymorphisms with Ischemic Stroke in a Greek Population. Stroke Res Treat. 2011; 2011(920584.
38. Sadikova RI, Nasibullin TR, Timasheva YR, Tuktarova IA, Erdman VV, Shein MI, et al. Allelic Combinations of Immune Response Genes and Risk of Development of Myocardial Infarction.

Russian Journal of Genetics. 2018; 54(4):472-481.

39. Bodine SC, Latres E, Baumhueter S, Lai VKM, Nunez L, Clarke BA, et al. Identification of ubiquitin ligases required for skeletal muscle atrophy. Science. 2001; 294(5547):1704-1708.
40. D'Hulst G, Jamart C, Van Thienen R, Hespel P, Francaux M, Deldicque L. Effect of acute environmental hypoxia on protein metabolism in human skeletal muscle. Acta Physiologica. 2013; 208(3):251-264.
41. Chaillou T, Koulmann N, Simler N, Meunier A, Serrurier B, Chapot R, et al. Hypoxia transiently affects skeletal muscle hypertrophy in a functional overload model. American Journal of Physiology-Regulatory Integrative and Comparative Physiology. 2012; 302(5):R643-R654.
42. Zaglia T, Milan G, Ruhs A, Franzoso M, Bertaggia E, Pianca N, et al. Atrogin-1 deficiency promotes cardiomyopathy and premature death via impaired autophagy. Journal of Clinical Investigation. 2014; 124(6):2410-2424.
43. Riksen NP, Stienstra R. Metabolism of innate immune cells: impact on atherosclerosis. Curr Opin Lipidol. 2018; 29(5):359-367.
44. Campolo J, Vozzi F, Penco S, Cozzi L, Caruso R, Domenici C, et al. Vascular injury post stent implantation: different gene expression modulation in human umbilical vein endothelial cells (HUVECs) model. PLoS One. 2014; 9(2):e90213.
45. Vozzi F, Campolo J, Cozzi L, Politano G, Di Carlo S, Rial M, et al. Computing of Low Shear Stress-Driven Endothelial Gene Network Involved in Early Stages of Atherosclerotic Process. Biomed Res Int. 2018; 2018(5359830.
46. Mahmoud AD, Ballantyne MD, Miscianinov V, Pinel K, Hung J, Scanlon JP, et al. The Human-Specific and Smooth Muscle Cell-Enriched LncRNA SMILR Promotes Proliferation by Regulating Mitotic CENPF mRNA and Drives Cell-Cycle Progression Which Can Be Targeted to Limit Vascular Remodeling. Circ Res. 2019; 125(5):535-551.
47. White SJ, Hayes EM, Lehoux S, Jeremy JY, Horrevoets AJ, Newby AC. Characterization of the differential response of endothelial cells exposed to normal and elevated laminar shear stress. J Cell Physiol. 2011; 226(11):2841-2848.
48. Doring Y, Manthey HD, Drechsler M, Lievens D, Megens RT, Soehnlein O, et al. Auto-antigenic protein-DNA complexes stimulate plasmacytoid dendritic cells to promote atherosclerosis. Circulation. 2012; 125(13):1673-1683.
49. Steenman M, Espitia O, Maurel B, Guyomarch B, Heymann MF, Pistorius MA, et al. Identification of genomic differences among peripheral arterial beds in atherosclerotic and healthy arteries. Scientific Reports. 2018; 8(12.
50. Ritchie ME, Phipson B, Wu D, Hu Y, Law CW, Shi W, et al. limma powers differential expression analyses for RNA-sequencing and microarray studies. Nucleic Acids Res. 2015; 43(7):e47.
51. Yu GC, Wang LG, Han YY, He QY. clusterProfiler: an R Package for Comparing Biological Themes Among Gene Clusters. Omics-a Journal of Integrative Biology. 2012; 16(5):284-287.

52. Mi H, Huang X, Muruganujan A, Tang H, Mills C, Kang D, et al. PANTHER version 11: expanded annotation data from Gene Ontology and Reactome pathways, and data analysis tool enhancements. Nucleic Acids Res. 2017; 45(D1):D183-D189.
53. The Gene Ontology C. The Gene Ontology Resource: 20 years and still GOing strong. Nucleic Acids Res. 2019; 47(D1):D330-D338.
54. Kanehisa M, Sato Y. KEGG Mapper for inferring cellular functions from protein sequences. Protein Sci. 2020; 29(1):28-35.
55. Szklarczyk D, Gable AL, Lyon D, Junge A, Wyder S, Huerta-Cepas J, et al. STRING v11: protein-protein association networks with increased coverage, supporting functional discovery in genome-wide experimental datasets. Nucleic Acids Res. 2019; 47(D1):D607-D613.
56. Bader GD, Hogue CW. An automated method for finding molecular complexes in large protein interaction networks. BMC Bioinformatics. 2003; 4(2.
57. Robin X, Turck N, Hainard A, Tiberti N, Lisacek F, Sanchez JC, et al. pROC: an open-source package for R and S plus to analyze and compare ROC curves. Bmc Bioinformatics. 2011; 12(
58. Ginestet C. ggplot2: Elegant Graphics for Data Analysis. Journal of the Royal Statistical Society Series a-Statistics in Society. 2011; 174(245-245.
59. Hosmer DW, Lemeshow S. Applied Logistic Regression. 2nd ed. 2000:91-142.

Figures

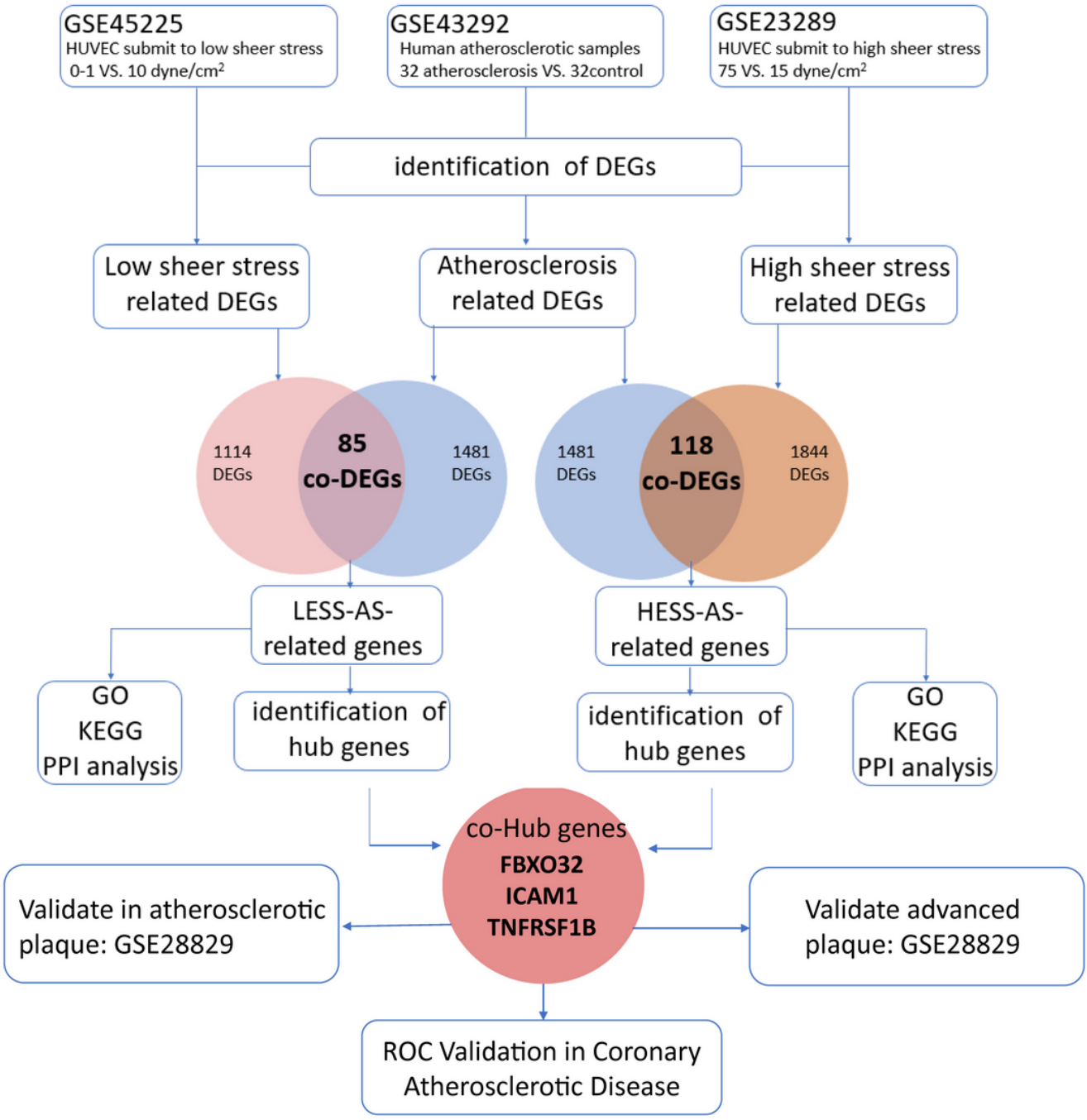

Figure 1

Workflow of bioinformatics analysis.

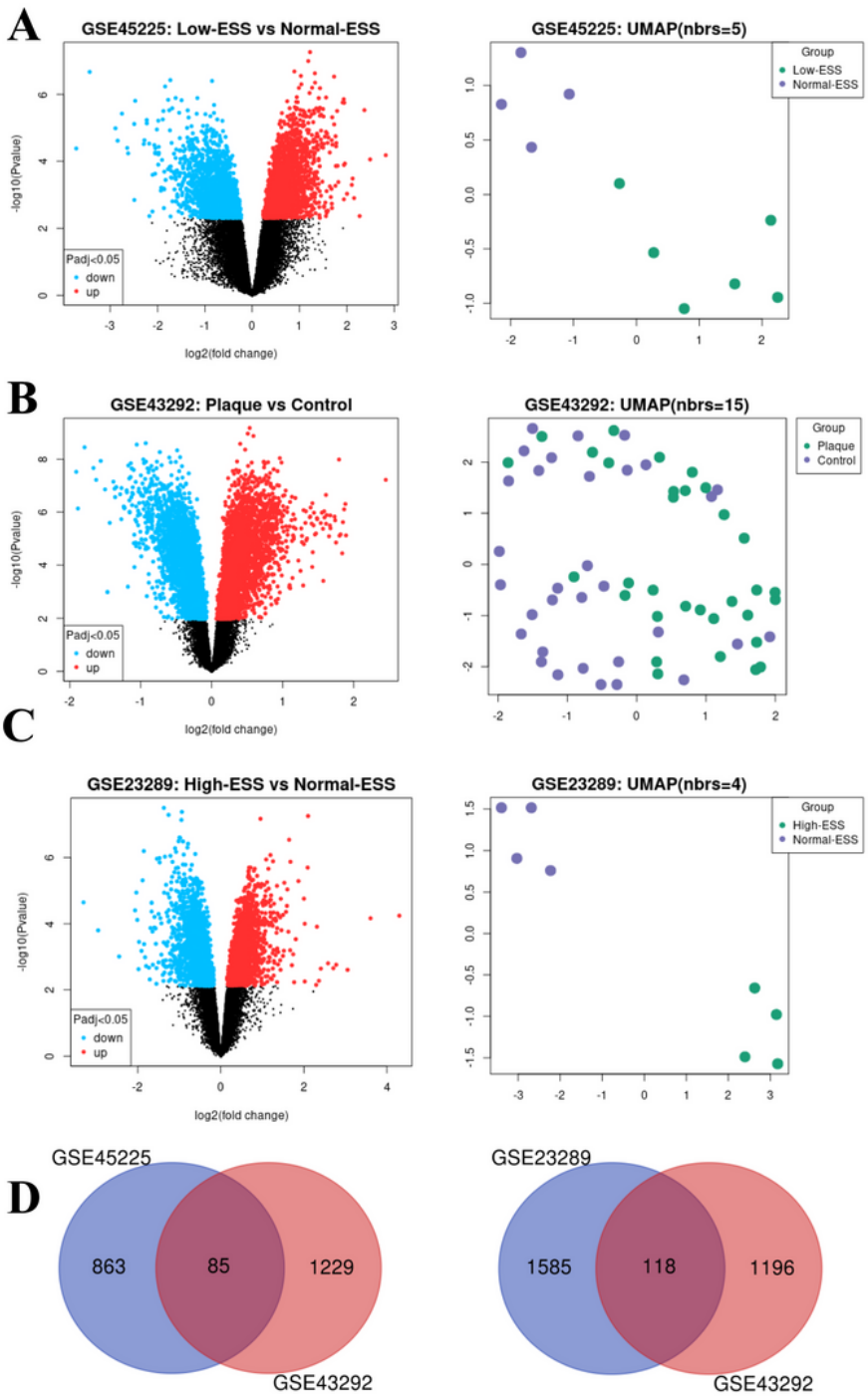

Figure 2

Identification of differential expressed genes (DEGs). (A) Volcanic map of 948 DEGs in low shear stress compared to those in physiological shear stress samples in GSE45225 dataset. The X axis represents the log2 (fold change) and the Y axis represents the p value. Blue to red color dots represents low to high expression level. The UMAP diagram shows the distinction between different samples. Each point in the figure represents a sample and the distance between samples represents the variation between samples.

(B) Volcanic plot of 1314 DEGs from GSE43292. We got the DEGs between plaque and control samples and the UMAP plot shows the distinction between different samples. (C) Volcanic plot of 1703 DEGs in high shear stress compared to those in physiological shear stress samples inGSE23289. (D) Venn diagrams showing the 85 overlapped genes in the GSE45225 and GSE43292 datasets, which were defined as LESS-AS-related genes. A total of 118 common DEGs were identified in GSE45225 and GSE43292 and defined as HESS-AS-related genes.

Figure 3

Gene Ontology (GO) analyses of LESS-AS-related genes in the biological processes (BPs), cellular components (CCs), and molecular functions (MFs). (A) Bubble plot of GO and KEGG: The x-axis represents the ratio of term genes to the total genes and y-axis represents the pathway term name. The size of dots represents the number of genes associated with the GO term, and the color corresponds to the P value. (B) Each go term is represented by a blue dot, the size of which reflects the number of genes associated with that term. Red dots represent genes linked to their assigned GO terms.

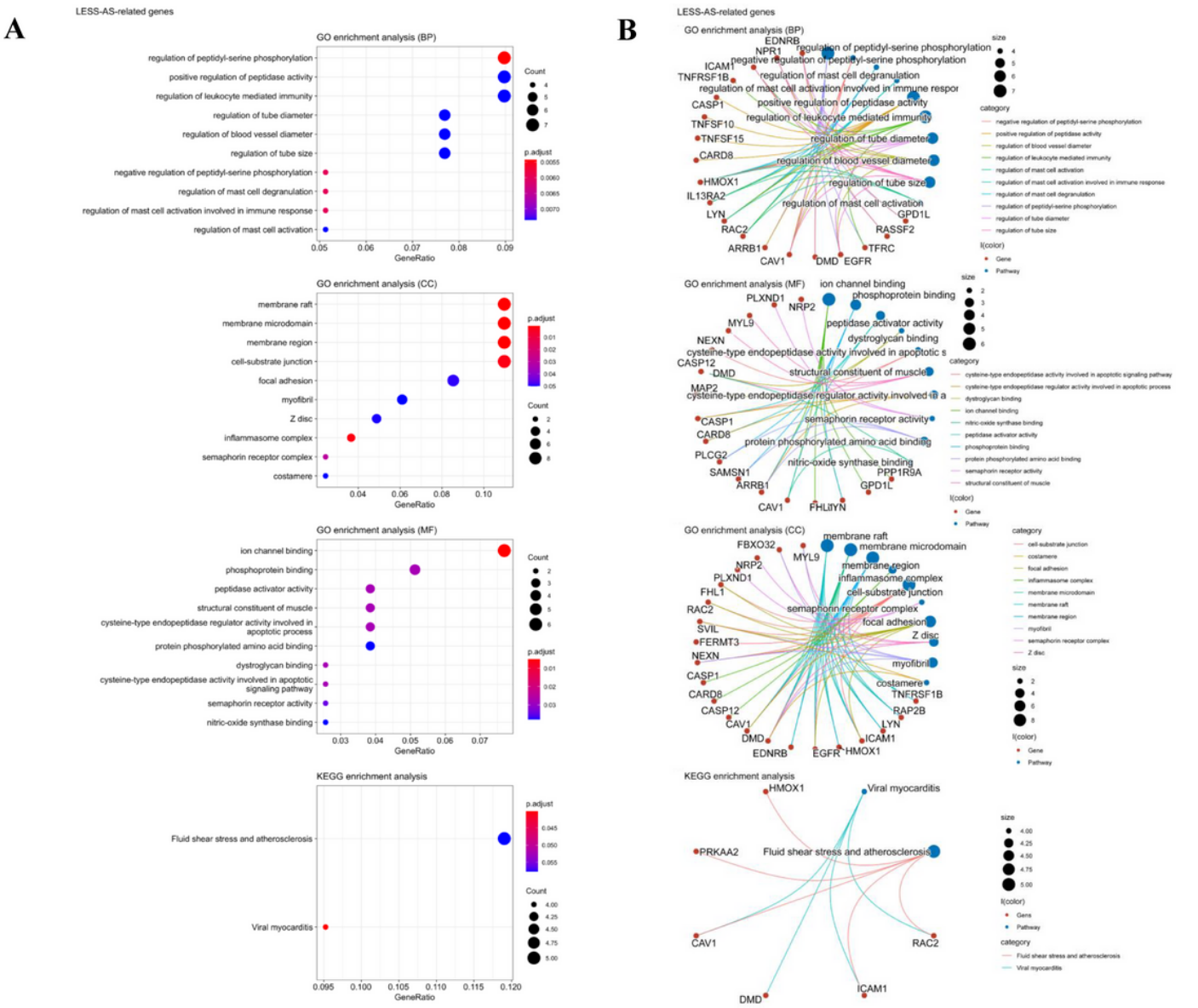

Figure 4

Gene Ontology (GO) analyses of HESS-AS-related genes in the biological processes (BPs) and cellular components (CCs). (A) Bubble plot of GO and KEGG: The x-axis represents the ratio of term genes to the total genes and y-axis represents the pathway term name. The size of dots represents the number of genes associated with the GO term, and the color corresponds to the P value. (B) Each go term is represented by a blue dot, the size of which reflects the number of genes associated with that term. Red dots represent genes linked to their assigned GO terms.

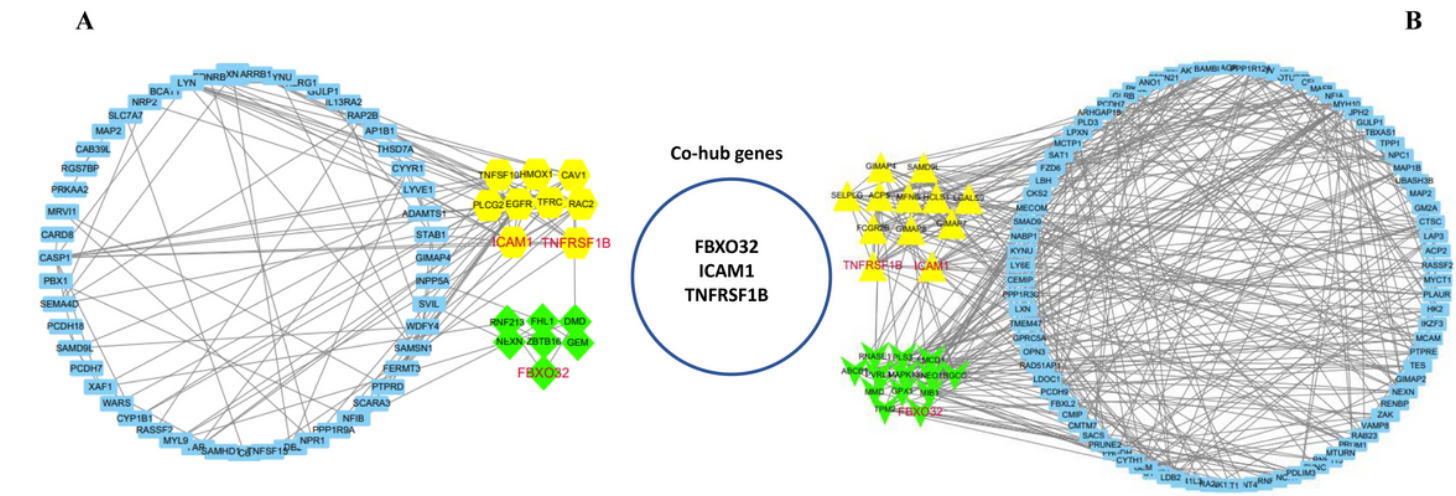

Figure 5

Identification of common hub genes in abnormal ESS and atherosclerotic plaque. (A) The PPI network of LESS-AS-related genes were constructed by the STRING online database. The sub-networks were identified by Cytoscape MCODE algorithm. The yellow and green dots represent the hub genes identified by the MCODE algorithm. (B) The PPI network of LESS-AS-related genes. The yellow and green dots represent densely connected network and hub genes identified by the MCODE algorithm in Cytoscape.

Figure 6

The expression levels of common hub genes in the GSE43292, GSE100921 and GSE28829 datasets. *** $P < 0.001$ (A) The expression levels of FBXO32, ICAM1 and TNFRSF1B between the atheroma plaque and intact tissue in GSE43292. (B) The expression levels of common hub genes between the atheroma plaque and control tissue in the GSE100927. (C) The expression levels of common hub genes between advanced plaque and early plaque in the GSE28829. * $P = 0.049$.

Figure 7

Receiver operating characteristic (ROC) analysis to assesses the ability of these common hub genes to distinguish samples of atherosclerotic plaque from normal arterial: (A) FBXO32 (AUC=0.782) (B) ICAM1 (AUC=0.822) (C) TNFRSF1B (AUC=0.801). (D) The combination of three indexes improved the sensitivity and specificity of prediction accuracies (AUC = 0.824).

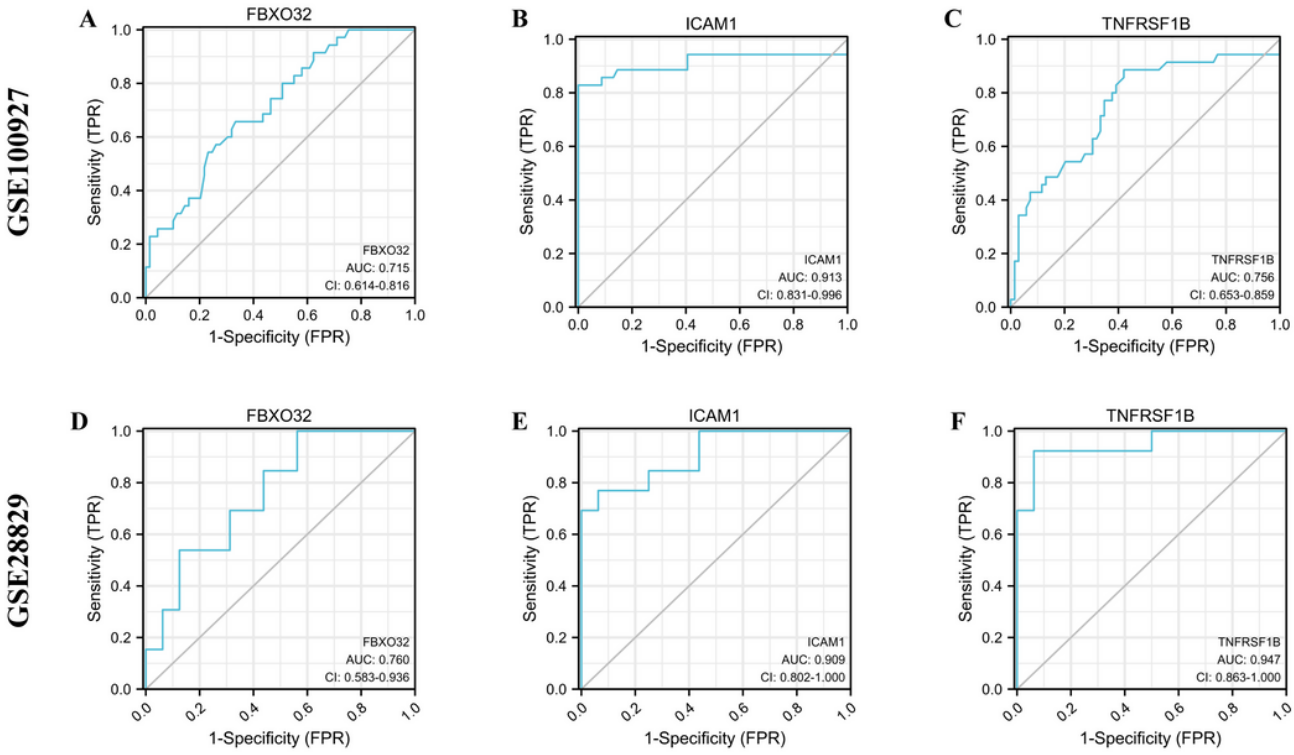

Figure 8

Receiver operating characteristic (ROC) analysis of these common hub genes in GSE100927 and GSE28829. (A, B, C) ROC analysis to assess the ability of these common hub genes to distinguish samples of atherosclerotic plaque from normal arterial in GSE100927. FBXO32 (AUC=0.715), ICAM1 (AUC=0.913), TNFRSF1B (AUC=0.756). (D, E, F) ROC analysis to assesses the ability of these common hub genes to distinguish samples of advanced plaque from early plaque in GSE28829: FBXO32 (AUC=0.760), ICAM1 (AUC=0.909), TNFRSF1B (AUC=0.947).